Alzheimer's Ab42 oligomers but not fibrils simultaneously bind to and cause damage to ganglioside containing lipid membranes

Thomas L Willliams, Benjamin R.G Johnson, Brigita Urbanc, Toby A Jenkins, Simon D.A Connell, Louise C Serpell

▶ **To cite this version:**

Thomas L Willliams, Benjamin R.G Johnson, Brigita Urbanc, Toby A Jenkins, Simon D.A Connell, et al.. Alzheimer's Ab42 oligomers but not fibrils simultaneously bind to and cause damage to ganglioside containing lipid membranes. Biochemical Journal, 2011, 439 (1), pp.67-77. 10.1042/BJ20110750 . hal-00628668

HAL Id: hal-00628668
https://hal.science/hal-00628668

Submitted on 4 Oct 2011

HAL is a multi-disciplinary open access archive for the deposit and dissemination of scientific research documents, whether they are published or not. The documents may come from teaching and research institutions in France or abroad, or from public or private research centers.

L'archive ouverte pluridisciplinaire **HAL**, est destinée au dépôt et à la diffusion de documents scientifiques de niveau recherche, publiés ou non, émanant des établissements d'enseignement et de recherche français ou étrangers, des laboratoires publics ou privés.

Biochemical Journal Immediate Publication. Published on 24 Jun 2011 as manuscript BJ20110750

Alzheimer's Aβ42 oligomers but not fibrils simultaneously bind to and cause damage to ganglioside containing lipid membranes

Abbreviated title: Binding and effect of Aβ42 oligomers on membranes

Thomas L. Williams*, Benjamin R. G. Johnson†, Brigita Urbanc‡, A. Toby A. Jenkins§, Simon D. A. Connell† and Louise C. Serpell*.

* School of Life Sciences, University of Sussex, Falmer, East Sussex, BN1 9QG, UK
†Institute for Molecular Biophysics, School of Physics and Astronomy, University of Leeds, Leeds, LS2 9JT, UK
‡Physics Department, Drexel University, Philadelphia, PA 19104, USA
§ Department of Chemistry, University of Bath, Bath, BA2 7AY, UK

Corresponding author: Prof Louise C Serpell, John Maynard-Smith Building, School of Life Sciences, University of Sussex, Falmer, East Sussex, BN1 9QG, UK. E-mail: L.C.Serpell@sussex.ac.uk. Telephone/Fax: +44 1273 877363

Current address: Dr Thomas Williams, Drexel University, Physics Department, 3141 Chestnut St, Philadelphia, PA 19104. USA.

THIS IS NOT THE VERSION OF RECORD - see doi:10.1042/BJ20110750

Accepted Manuscript

Licenced copy. Copying is not permitted, except with prior permission and as allowed by law.
© 2011 The Authors Journal compilation © 2011 Portland Press Limited

Biochemical Journal Immediate Publication. Published on 24 Jun 2011 as manuscript BJ20110750

THIS IS NOT THE VERSION OF RECORD - see doi:10.1042/BJ20110750

Abstract

Amyloid-Beta peptide (Aβ) assembles to form amyloid fibres that accumulate in senile plaques associated with Alzheimer's disease (AD). The major constituent, a 42-residue Aβ peptide, has the propensity to assemble and form soluble and potentially cytotoxic oligomers as well as ordered, stable amyloid fibres. It is widely believed that the cytotoxicity is a result of the formation of transient soluble oligomers. This observed toxicity maybe associated with the ability of oligomers to associate with and cause permeation of lipid membranes. Here, we have investigated the ability of oligomeric and fibrillar Aβ42 to simultaneously associate with and affect the integrity of biomimetic membranes *in vitro*. Surface Plasmon field enhanced Fluorescence spectroscopy reveals that the binding of the freshly dissolved, oligomeric 42-residue peptide binds with a two-step association with the lipid bilayer and causes disruption of the membrane resulting in leakage from vesicles. In contrast, fibrils bind with a 2-fold reduced avidity and their addition results in around 2-fold less fluorophore leakage compared to oligomeric Aβ. Binding of the oligomers may be in part mediated by the GM1 ganglioside receptors showing a 1.8-fold increase in oligomeric Aβ binding and a 2-fold increase in permeation compared to when GM1 is not present. Atomic Force Microscopy reveals the formation of defects and holes in response to oligomeric Aβ, but not preformed fibrillar Aβ. Our results indicate significant membrane disruption arises from association of low molecular weight Aβ and this may be mediated by mechanical damage to the membranes by Aβ aggregation. This membrane disruption may play a key role in the mechanism Aβ-related cell toxicity in Alzheimer's disease.

Keywords: Amyloid-β peptide, GM1 Ganglioside, Membrane Bilayers, Alzheimer's, Protein Misfolding, Atomic Force Microscopy, Surface Plasmon field-enhanced Fluorescence Spectroscopy.

Abbreviations: Aβ, amyloid-β peptide; Aβ40, amyloid-β peptide1-40; Aβ42, amyloid-β peptide1-42; AD, Alzheimer's disease; AFM, Atomic Force Microscopy; Alexa Fluor 647, Alexa Fluor 647 carboxylic acid, succinimidyl ester dye; APP, amyloid precursor protein; Biotinyl Cap PE, 1,2-dipalmitoyl-*sn*-glycero-3-phosphoethanolamine-N-(cap biotinyl); Biotin-thiol, 11-mercaptoundecanoic-(8-biotinoylamido-3,6-dioxaoctyl)amide; D*, apparent dye diffusion coefficient; DMPC, 1,2-dimyristoyl-*sn*-glycero-3-phosphocholine; DMPE, 1,2-dimyristoyl-*sn*-glycero-3-phosphoethanolamine; DMPG, 1,2-dimyristoyl-*sn*-glycero-3-phospho-(1'-rac-glycerol); DMPS, 1,2-dimyristoyl-*sn*-glycero-3-phospho-L-serine; DPPC, 1,2-dipalmitoyl-*sn*-glycero-3-phosphocholine; DPPG, 1,2-dipalmitoyl-*sn*-glycero-3-phospho-(1'-*rac*-glycerol); GM1, monosialoganglioside G_{M1}; HEPES, 4-(2-Hydroxyethyl)piperazine-1-ethanesulfonic acid, N-(2-Hydroxyethyl)piperazine-N′-(2-ethanesulfonic acid); HFIP, 1,1,1,3,3,3-hexafluoro-2-propanol; K_D, Equilibrium dissociation constant; LUV, large unilamellar vesicles; PE, Phosphatidylethanolamine; POPC, 1-palmitoyl-2-oleoyl-*sn*-glycero-3-phosphocholine; POPG, 1-palmitoyl-2-oleoyl-*sn*-glycero-3-phospho-(1'-*rac*-glycerol); [R]%, percentage reflectivity; R_{eq}, equilibrium response; R_{max}, maximum response; RPM, revolutions per minute; RSM % E, Root Square Mean % Error; SAM, Self-Assembled Monolayer; SFL6, SCHOTT SFL6

Accepted Manuscript

Licenced copy. Copying is not permitted, except with prior permission and as allowed by law.
© 2011 The Authors Journal compilation © 2011 Portland Press Limited

Biochemical Journal Immediate Publication. Published on 24 Jun 2011 as manuscript BJ20110750

optical glass; SPFS, Surface Plasmon field-enhanced Fluorescence Spectroscopy; SPR, Surface Plasmon Resonance; SUV, small unilamellar vesicles; tBLMs, tethered bilayer lipid membranes.

Accepted Manuscript

THIS IS NOT THE VERSION OF RECORD - see doi:10.1042/BJ20110750

Licenced copy. Copying is not permitted, except with prior permission and as allowed by law.
© 2011 The Authors Journal compilation © 2011 Portland Press Limited

Biochemical Journal Immediate Publication. Published on 24 Jun 2011 as manuscript BJ20110750

THIS IS NOT THE VERSION OF RECORD - see doi:10.1042/BJ20110750

Introduction

Alzheimer's disease (AD) is the most prevalent cause of dementia, with estimates of between 18-30 million sufferers worldwide [1]. AD is characterized by the deposition of intraneuronal neurofibrillary tangles, extracellular amyloid-containing neuritic plaques composed predominantly of fibres formed from Aβ and the presence of cerebrovascular amyloid fibres [2]. Aβ is processed from the integral membrane protein, the Amyloid Precursor Protein (APP) to produce predominantly Aβ40 or Aβ42. Aβ42 is known to be the more fibrillogenic and toxic form of Aβ, and an increased ratio of Aβ42 to 40 is associated with familial forms of Alzheimer's disease [3]. *In vitro*, Aβ assembles to form small, pre-fibrillar oligomers and over time, fibrils, and the assembly state has been shown to modulate the cellular toxicity of the peptide [4]. Aβ-membrane interactions may play a key role in the observed Aβ toxicity associated with Alzheimer's disease and assist the entry of the Aβ peptide into the cytoplasm of the cell (see associated paper). The influence of both Aβ40 and 42 assemblies on model membranes with varying compositions have been studied previously [4-8], although the majority have focused on the less disease related form, Aβ40. These studies have shown that Aβ may cause partial disruption of lipid membranes [5, 7-9]. However, significant advances have been made in the last few years to ensure disaggregated, solvent free peptide [10, 11]. We have previously shown that the ability of Aβ42 peptide to disrupt the integrity of biomimetic vesicles decreases as the peptide assembles to form mature fibres, and it is therefore clear that the assembly state of the peptide plays an important role in the toxic ability [12].

The effect of the Aβ peptide has been linked to membrane composition, with both cholesterol [13] and GM1 gangliosides being implicated in mediating the affect of the peptide [14-16]. Gangliosides are glycosphingolipids composed of a hydrophilic sialic acid moiety exposed to the external environment and a hydrophobic membrane-embedded ceramide moiety. Their inclusion in membranes is typically around 2 mol % of cellular membranes, [17] but this can vary between 0.5-13% w/w depending on cell type and during the development of the cell [18-20]. Interactions between the GM1 and Aβ are believed to involve hydrophobic and electrostatic interactions, as greater affinity is observed between Aβ and the hydrophobic membrane-embedded ceramide portion of GM1 compared to its affinity with the hydrophilic sialic acid portion [15]. GM1 is also implicated in seeding assembly of the Aβ associated with the membrane [14] and has been shown to mediate binding of Aβ1-40 [21].

We have previously used biomimetic unilamellar vesicles in solution to monitor the effect of Aβ aggregation state on the ability to cause membrane permeation using a calcein release assay. We demonstrated that as the Aβ peptide assembles from an oligomeric to fibrillar state, the ability to cause membrane permeation decreases [12]. We also showed that the

Accepted Manuscript

Licenced copy. Copying is not permitted, except with prior permission and as allowed by law.
© 2011 The Authors Journal compilation © 2011 Portland Press Limited

Biochemical Journal Immediate Publication. Published on 24 Jun 2011 as manuscript BJ20110750

removal of GM1 from the bilayer vesicles significantly decreases the ability of Aβ42 to permeate the membranes. In support of this, Ying *et al* [22] and Müller *et al* [23] showed an effect on membrane fluidity by the addition of Aβ, showing Aβ specifically altered the acyl chain layer of cell membranes while the polar head group layer was much less affected [23, 24]. Other amyloidogenic peptides, such as IAPP have also been shown to affect the integrity of lipid membranes [25, 26].

Here, we have examined the binding and effect of small Aβ42 assemblies on biomimetic membranes simultaneously for the first time. Surface Plasmon field-enhanced Fluorescence Spectroscopy (SPFS) is a technique that combines the ability of SPR to monitor adsorption and desorption events at the air/dielectric interface with the ability to resonantly excite fluorescent molecules within the evanescent field extending 200 nm within the dielectric, and this allows us to simultaneously observe both Aβ-membrane interactions and correlate with permeation events. SPFS has previously been used to monitor the tethering of intact Large Unilamellar Vesicles (LUVs) to a functionalized gold substrate and the events following the addition of the membrane lysing protein, phospholipase A_2 [27] and membrane permeation caused by cholera toxin [28]. Permeation is the term we apply here to mean the penetration of the lipid bilayer by the Aβ peptide resulting in a non-continuous membrane surface and the emergence of defects/holes or deformations within the bilayer to allow increased diffusion across the membrane bilayer. Aβ oligomers are the term we apply in this study to mean freshly dissolved peptide in biological buffer, that is soluble and show no defined fibrillar features.

In this study, we tether biotinylated LUVs to a biotinylated thiol Self-Assembled Monolayer (SAM) using streptavidin to covalently tether the biomimetic membranes to the functionalized surface (Supplementary Figure 1). We ensure complete construction of the functionalized surface and tethering of the biotinylated LUVs by monitoring with SPR. SPR coupled with SPFS is then used to monitor adsorption of the Aβ peptide to the tethered membrane surface concurrent with monitoring the change in fluorescence intensity as a result of fluorescent dye diffusion through membranes. Analysis of peptide-membrane binding kinetics is performed using a Langmuir binding isotherm to determine the equilibrium dissociation constant and fitting the data to an exponential function to analyze differences between oligomeric and fibrillar Aβ binding. The fluorescence leakage is modeled using a simple diffusion model. Using these techniques, we aim to simultaneously reveal the interactions between Aβ42, the physiologically relevant variant implicated in Alzheimer's disease, with permeation of biomimetic membranes. SPFS with tethered LUVs is used to compare the adsorption of oligomeric and fibrillar Aβ42 to the membrane surfaces whilst simultaneously monitoring the permeation of the lipid bilayers. We show that binding of the

THIS IS NOT THE VERSION OF RECORD - see doi:10.1042/BJ20110750

Accepted Manuscript

Licenced copy. Copying is not permitted, except with prior permission and as allowed by law.
© 2011 The Authors Journal compilation © 2011 Portland Press Limited

Biochemical Journal Immediate Publication. Published on 24 Jun 2011 as manuscript BJ20110750

peptide to the membrane is closely followed by membrane permeation, which has only been previously reported in separate studies. Further to this, we report the removal of the GM1 ganglioside from the bilayer membranes significantly reduces the binding of the oligomeric Aβ42, and results in decreased permeation of the membranes compared to when GM1 is present. This indicates that GM1 can modulate both binding of the peptide to the membrane as well mediating increased Aβ-induced permeation in a concentration dependent fashion. The fibrillization of the oligomeric peptide and the permeation of membranes were also visualized by atomic force microscopy (AFM) revealing that administration of oligomeric Aβ42 resulted in visible holes within the lipid bilayer and permeation progresses through both leaflets of the bilayer over time. Our study reports key advances showing that: (*i*) oligomeric Aβ binds in a two-step process, whereby the specific adsorption of the peptide precedes permeation of the membranes, and permeation typically begins within the first phase of peptide association, while fibrillar Aβ binds in a one-step association (*ii*) ensuring all pre-disaggregation solvents are carefully removed before addition to membranes ensures true and reliable binding constant determination, (*iii*) GM1 exclusion in the membranes reduces the association of Aβ to the membrane surface but has a much greater affect in modulating Aβ-induced permeation, and (*iv*) Aβ addition to bilayers can cause large, visible defects and holes within the membrane surface, as a possible consequence of altered membrane viscoelasticity.

Experimental Section

Amyloid peptides

Aβ(1-42) HFIP (referred to as Aβ42), >97% purity was purchased from rPeptide (Bogart, GA, USA). All peptides were used without further purification.

Peptide preparation

Aβ peptides require treatment to ensure disaggregation and removal of preaggregated species [11], Solvents including HFIP, DMSO and Trifluroethanol (TFE) have been shown to significantly affect amyloid assembly and cause membrane leakage [29]. The 1 $mg.mL^{-1}$ Aβ42 peptide was solubilized in 1,1,1,3,3,3-hexafluoro-2-propanol >99.0% (Fluka, Sigma-Aldrich Company Ltd, Dorset, UK), vortexed for 60 seconds and sonicated in a 50/60 *Hz* bath sonicator for 60 seconds. HFIP is initially used to break β-sheet structures and render the peptide α-helical. However HFIP, has also been shown to promote intramolecular hydrogen bonding networks so further processing is also needed [30]. Solvent was removed using dry nitrogen and vacuum desiccated for 30 minutes. The amyloid was re-solubilized at 1 $mg.mL^{-1}$ with dimethyl sulfoxide >99.9% (Sigma-Aldrich Company Ltd, Dorset, UK), vortexed vigorously for 60 seconds and sonicated for 60 seconds. DMSO is used as a proton acceptor to destroy the hydrogen bond network to maintain the peptide in its monomeric state. [31].

THIS IS NOT THE VERSION OF RECORD - see doi:10.1042/BJ20110750

Accepted Manuscript

Licenced copy. Copying is not permitted, except with prior permission and as allowed by law.
© 2011 The Authors Journal compilation © 2011 Portland Press Limited

Biochemical Journal Immediate Publication. Published on 24 Jun 2011 as manuscript BJ20110750

200 μL of the peptide in DMSO was added to a 2 mL HEPES pH 7.4 equilibrated Zeba™ desalt spin column, once absorbed into the column resin a 40 μL stacker of 0.22 μm filtered water was added to the column. The column was spun in a 4 ^{o}C controlled Mikro 22R centrifuge (Hettich UK, Manchester, UK) at 1000 g for 2 minutes. The eluted peptide was centrifuged in a 4 ^{o}C controlled Eppendorf microcentrifuge (Eppendorf UK Ltd, Cambridge, UK) at 16,000 g for 30 minutes to remove contaminants and pre-formed fibrillar material. The supernatant was placed in a clean non-stick microcentrifuge tube and stored at 4 ^{o}C. The concentration was determined using a molar extinction coefficient of 1490 $M^{-1}cm^{-1}$ and the absorbance was measured at a wavelength of 280 nm using an Eppendorf Biophotometer (Eppendorf UK Ltd, Cambridge, UK) and resulted in peptide concentrations of 100-130 μM. The peptide stock was diluted to the 10 μM working concentration for all experiments. For the preparation of Aβ42 fibres, the oligomeric Aβ42 was statically incubated at 21 ^{o}C in a temperature controlled Eppendorf Thermomixer Comfort (Eppendorf, UK Ltd) and incubated for 7 days. Complete removal of HFIP and DMSO, was previously demonstrated in our recent work [12] to prevent the continued influence of the solvents on Aβ secondary structure and assembly kinetics [29].

Biomimetic membrane constituents

1,2-dimyristoyl-*sn*-glycero-3-phosphocholine (DMPC), 1,2-dimyristoyl-*sn*-glycero-3-phosphoethanolamine (DMPE), 1,2-dimyristoyl-*sn*-glycero-3-phospho-(1'-rac-glycerol) (DMPG), and 1,2-dimyristoyl-*sn*-glycero-3-phospho-L-serine (DMPS) were purchased from Avanti Polar Lipid Inc (Alabaster, AL, US). Cholesterol, 95% and Monosialoganglioside G_{M1} from bovine brain, >95% lyophilized powder were purchased from Sigma-Aldrich Company Ltd (Dorset, UK). All materials were used without further purification.

For SPFS, 40 $mg.mL^{-1}$ stock solutions of the bilayer constituents were solubilized in 2:1 (v/v) chloroform/methanol in a glass vial from the stock solutions (see table 1 for compositions) and the solvent was removed using dry nitrogen, and vacuum desiccated over night. The lipid films were rehydrated with 5 μM Alexa Fluor 647® Succinimidyl Ester (Molecular Probes, Invitrogen Ltd, UK), hydrolysed to form the carboxylic acid and dissolved in 10 mM HEPES, 100 mM NaCl, 1 mM EDTA, and 0.05 mM NaN_3 (all purchased from Sigma-Aldrich Company Ltd, Dorset, UK), and referred to as HEPES pH 7.4, and vortexed vigorously for 30 minutes. The resulting suspension was passed 19 times through an Avestin extruder fitted with two stacked 100 nm polycarbonate membranes (GC Technology Ltd, Bedford, UK). For GM1-deficient LUV composition see Table 1.

For AFM bilayer composition see Table 1. The lipid films were rehydrated with HEPES pH 7.4, and vortexed vigorously for 30 minutes. The resulting suspension was passed 19 times

THIS IS NOT THE VERSION OF RECORD - see doi:10.1042/BJ20110750

Accepted Manuscript

Licenced copy. Copying is not permitted, except with prior permission and as allowed by law.
© 2011 The Authors Journal compilation © 2011 Portland Press Limited

Biochemical Journal Immediate Publication. Published on 24 Jun 2011 as manuscript BJ20110750

through an Avestin extruder fitted with two stacked 100 nm polycarbonate membranes (GC Technology Ltd, Bedford, UK).

Bilayer Preparation

For SPFS, clean high refractive index glass (SFL6, n = 1.7988, UQG Optics Ltd) was coated with a thin ~50 nm gold layer (99.99 %, Advent Research Materials Ltd) using an Emitech K975 thermal evaporator. The gold was thermally annealed at 500 ^{o}C for ninety seconds. The gold-coated wafers were ozone cleaned in a UV TipCleaner for ten minutes and then placed in absolute ethanol for 10 minutes and dried with nitrogen to ensure a clean surface. 11-mercaptoundecanoic-(8-biotinoylamido-3,6-dioxactly)amide [32], and subsequently referred to as biotin-thiol was self-assembled in an ethanolic solution of 0.05 mM biotin-thiol and 0.95 mM 11-mercapto-1-undecanol (99 %, Sigma) to form a self-assembled monolayer onto the gold substrates for 16 hours. The biotin surface was coupled with streptavidin (500 nM in HEPES pH 7.4), to create the 'capture' surface for the biomimetic lipid vesicles. After LUV attachment the system was rinsed with buffer to remove no encapsulated fluorophore and non-bound vesicles from the system, the experimental setup is shown in supplementary Figure 1.

For AFM, 200 µL of 1mg.mL^{-1} LUVs were adsorbed to mica and incubated at room temperature for 3 hours. The formed bilayer was rinsed with 10 mM $MgCl_2$ for 10 minutes to facilitate complete vesicle rupture, and then rinsed in HEPES pH 7.4.

Surface Plasmon Resonance (SPR) and Surface Plasmon field-enhanced Fluorescence Spectroscopy (SPFS) Measurements and Data Analysis.

SPR was used to follow the construction of the modified surface, and the experimental setup has been previously described [33, 34]. The surface construction was monitored as a change in reflectivity angle scan, from which the mass adsorption can be calculated from a simple empirical relationship of Adsorption (A) = $\Delta\theta/(\Delta\theta/\sigma)$ where $\Delta\theta$ is the resonance minimum and $\Delta\theta/\sigma$ is the surface concentration correlation (0.1868^{o}). The surface construction and adsorption/desorption events following Aβ addition to the membrane surface was also followed kinetically as the change in reflection intensity at an angle of around 1.5 ^{o} lower than the resonance angle. Therefore, changes in the reflected light intensity at a fixed angle allow real-time measurements of peptide-membrane binding. The equilibrium dissociation constant (K_D) is fitted to the binding isotherm ($R_{eq} = R_{max}[A]/(k_{off}/k_{on})[A])$, where R_{eq} is the equilibrium response, R_{max} is the maximum signal response, [A] is the analyte concentration, k_{off} is the dissociation rate constant and k_{on} is the association rate constant) using Origin 7

THIS IS NOT THE VERSION OF RECORD - see doi:10.1042/BJ20110750

Accepted Manuscript

Licenced copy. Copying is not permitted, except with prior permission and as allowed by law.
© 2011 The Authors Journal compilation © 2011 Portland Press Limited

Biochemical Journal Immediate Publication. Published on 24 Jun 2011 as manuscript BJ20110750

data analysis software (OriginLab, Northampton, MA, USA). The equilibrium dissociation constant (K_D) was determined, and all changes in reflectivity were normalized.

Aβ-membrane response was also analysed using an exponential functional expression to determine mono-, bi- and/or tri-phasic association of the oligomeric and fibrillar Aβ with the membrane. Using the expression $y(t) = a_0 + a_1 (1 - \exp(-t/t1)) + a_2 (1 - \exp(-t/t2)) + a_3 (1 - \exp(-t/t3))$ derived from $1 - \exp(-t/t1)$. Where t_1 , t_2, and t_3 = time scale associated with the mono-, bi-, and triphasic processes respectively, which is equal to 0 at $t = 0$ and goes to 1 when $t = \infty$, a_1, a_2, and a_3 = constant factor for amplitude of observed change for the mono-, bi- and tri-phasic exponential function respectively, and a_0 = time correction factor for y value as y does not = 0, using Grace-5.1.22 (Cambridge, MA, USA).

The evanescent wave is used to resonantly excite fluorescence dye molecules within 200 nm of the surface and will be detected by a photomultiplier tube, allowing us to monitor any emitted fluorescence encapsulated within the membrane vesicles but not in the bulk solution. A simple theoretical model based on Fick's first law of diffusion was used to fit the decrease in fluorescence-time curves obtained following Aβ induced membrane permeation as previously used to model cholera-membrane interactions [28]. The fluorophore flux through permeated membranes is calculated as the apparent dye diffusion coefficient (D^*), is effectively determined from the gradient of the linearized change in fluorescence over time, and takes into account vesicle membrane internal volume and membrane area and thickness. Therefore, D^* is not a function of total encapsulated fluorescent molecules lost from the vesicle aqueous space, but the extrapolated linerarized slope of the dye diffusion rate. To be clear, the fluorescence scale shown in Figure 2 is arbitrary and the changes in fluorescence between experiments cannot be compared directly to each other, these fluorescence traces are extrapolated and processed using Origin analysis software, therefore apparent dye diffusion coefficient *(D^*)* provides a direct means of comparing permeation rates.

The experiments were performed in duplicate (Supplementary figure 4) and the kinetic traces shown in Figure 2 are representative of each experiment. Initially, we monitored the construction of the functionalized surface by following the angle-resolved SPR reflectivity curves (Supplementary Figure 2) and the change in resonance minima allowed us to calculate the change in mass to the surface (Supplementary Table 1). Scanning electron microscopy was employed to confirm the covalent attachment of whole, intact lipid vesicles (Figure 1a).

Atomic Force Microscopy Measurements

THIS IS NOT THE VERSION OF RECORD - see doi:10.1042/BJ20110750

Accepted Manuscript

Licenced copy. Copying is not permitted, except with prior permission and as allowed by law.
© 2011 The Authors Journal compilation © 2011 Portland Press Limited

Biochemical Journal Immediate Publication. Published on 24 Jun 2011 as manuscript BJ20110750

All bilayer images were obtained under filtered HEPES pH 7.4 buffer using a Nanoscope IV Multimode AFM (Veeco CA). Bilayer formation was verified by imaging defects and classic bilayer morphology (4.8-5.0 nm step heights for this bilayer composition), or a series of force-distance curves and a complete force-volume map. Aβ42 solution was injected into the liquid cell via flexible tubing so as not to disturb the imaging process too greatly (although the change in temperature often necessitated a resetting of scan parameters). A flexible gasket was used to seal the liquid cell to prevent evaporation and maintain buffer concentration, and allow for overnight incubations if necessary. Temperature was not directly controlled, although the laboratory temperature was stable, and the cell temperature equilibrated to 26°C. Both contact mode and tapping mode were used throughout, using a selection of Veeco NP cantilevers depending upon mode. Images were processed using Nanoscope v5.12r30 software. Area measurements were performed using the Bearing Analysis function.

Transmission electron microscopy

Electron micrograph images of Aβ were prepared as previously described [12]. Briefly, 4 μl droplet of the peptide solution was adsorbed onto formvar/carbon coated 400 mesh copper grids (Agar Scientific, Essex, UK) for 60 seconds, and blotted dry. 4 μl of 0.22 μm filtered water was added to the grid and immediately blotted, then negatively stained with 4 μl of 2% w/v uranyl acetate for 60 seconds and blotted dry. The grid was allowed to air dry before examination on a Hitachi 7100 microscope (Hitachi, Germany) fitted with a Gatan Ultrascan 1000 CCD camera (Gatan, Abingdon, UK). Aliquots of samples at the stock concentration were taken at time points for each experiment to monitor fibrillization state and morphology. Measurements were made using ImageJ [35].

Scanning electron microscopy

100 nm LUVs were tethered to the biotinylated-thiol SAM as described above for the SPFS measurements, then the glass substrate removed from the flow-cell. The tethered LUVs were fixed by immersion in 2 % glutaraldehyde solution (25 % EM grade, Agar Scientific Ltd) for 30 minutes. The fixed LUVs were then immersed in a 1 % osmium tetraoxide solution (2% solution, Agar Scientific Ltd) for 20 minutes to biologically fix and stain the sample. The substrate was rinsed carefully with HEPES pH 7.4 and air dried before examination on a JEOL JSM6310 microscope (JEOL, UK Ltd).

THIS IS NOT THE VERSION OF RECORD - see doi:10.1042/BJ20110750

Accepted Manuscript

Licenced copy. Copying is not permitted, except with prior permission and as allowed by law.
© 2011 The Authors Journal compilation © 2011 Portland Press Limited

Biochemical Journal Immediate Publication. Published on 24 Jun 2011 as manuscript BJ20110750

Results and Discussion

Transmission electron microscopic characterization of Aβ42

The assembly characteristics of Aβ42 were monitored using transmission electron microscopy, Aβ42 used immediately following disassembly treatment is from now on referred to as "0-hour incubated Aβ". 0-hour incubated Aβ shows a variety of morphological species including small circular peptide between 10-20 nm in diameter, 30-50 nm annular structures, larger 60-70 nm curvilinear oligomers, and 70-140 nm amorphous peptide assemblies (Figure 1b). At 20-hours the peptide forms long, twisted, unbranched, and straight fibres with defined edges (Figure 1c). We have previously shown that Aβ42 was capable of forming morphologically indistinguishable fibres when grown in the presence of lipid membranes, and LUVs changed from regular spherical 100 nm diameter lipid vesicles with apparently smooth bilayers to irregularly shaped, rough vesicles where the bilayer began to bleb and swell in the presence of Aβ42 [12].

Oligomeric Aβ42-Membrane Interaction Characterization

Monitoring the Oligomeric Aβ42-Membrane Interactions by SPFS

The association of different bound Aβ assemblies with membranes and their subsequent effect on biomimetic membrane stability was followed by SPR and SPFS both as changes in resonance angle shifts, reflected light intensity and fluorescence intensity. The experiments were performed in duplicate (supplementary figure 4) and the kinetic traces shown in Figure 2 are representative of each experiment. Initially, we monitored the construction of the functionalized surface by following the angle-resolved SPR reflectivity curves (Supplementary Figure 2) and the change in resonance minima allowed us to calculate the change in mass to the surface (Supplementary Table 1). Scanning electron microscopy was employed to confirm the covalent attachment of whole, intact lipid vesicles (Figure 1a). As a control, we re-circulated HEPES pH 7.4 buffer containing no peptide into the flow-cell for 18 hours to monitor the stability of the tethered LUVs. The passive diffusion of the Alexa Fluor 647 through the membranes was calculated as the apparent dye diffusion coefficient, $D^* = 7.29 \times 10^{-22}$ $m^2.sec^{-1}$ (Supplementary Figure 3) and this serves as a baseline.

For the purposes of the following experiments, we have selected a concentration of 10 μM Aβ to ensure a visible affect between Aβ-membrane interactions in the time course of our studies. This is comparable to concentrations that show a significant toxic effect on neuroblastomas cells (see accompanying paper). An Aβ concentration titration was initially performed and maximal peptide-membrane binding was observed at this peptide concentration (data not shown). 10 μM 0-hour incubated Aβ42 was injected into the flow-cell using a peristaltic pump at a flow rate of 1.8 $mL.min^{-1}$ to ensure continuous delivery of the

THIS IS NOT THE VERSION OF RECORD - see doi:10.1042/BJ20110750

Accepted Manuscript

Licenced copy. Copying is not permitted, except with prior permission and as allowed by law.
© 2011 The Authors Journal compilation © 2011 Portland Press Limited

Biochemical Journal Immediate Publication. Published on 24 Jun 2011 as manuscript BJ20110750

sample to the membrane surface and minimize mass transfer effects. An increase in reflectivity was observed within 10 minutes as a result of Aβ42 binding to the membrane surface (Figure 2a, primary y-axis). The peptide proceeds to reach an initial equilibrium within the first 60 minutes as there is a short plateau in normalized Reflectivity [R]% during Aβ binding at this time, which results from the specific association of the oligomeric Aβ42 with the LUVs. Over the subsequent 400 minutes there is a second phase of peptide binding. This biphasic interaction suggests an initial period of specific adsorption for the first 60 minutes, which is then followed by a slower phase of association. After equilibrium was reached the system was washed with fresh buffer (after around 500 minutes), whereby the Reflectivity [R]% drops which is indicative of non-specifically or weakly bound peptide being washed into solution. From rinse-off data the dissociation constant can be calculated (see experimental section). An angle resolved reflectivity scan was performed to measure the shift in resonance minima, where it is calculated that there is a 0.59 $ng.mm^{-2}$ increase in mass at the supported surface, and the K_D was calculated to be 2.68×10^{-8} M. Previous studies have reported SPR derived K_D constants for oligomeric Aβ42 to vesicles containing DMPC/GM1 of 5.2×10^{-7} M [16]. The discrepancy between K_D values is likely to be due to differences in bilayer composition and the method of Aβ preparation. In this study, we have prepared Aβ42 to ensure removal of preformed aggregates. The increased complexity of our membranes, which include physiologically relevant GM1, sterols and negatively charged phospholipids, tend to favour the association of Aβ with membranes, therefore, the determined K_D in this study suggest stronger binding compared to simpler membrane systems, and careful preparation to ensure all peptide disaggregation solvents are removed ensures no external influence in membrane binding occurs. At the end of the measurement 5g/L sodium dodecyl sulfate was added to the system to lyse all attached membrane vesicles and a change in resonance angle scan minimum was determined and showed 11.78 $ng.mm^{-2}$ of material was lost from the surface, showing the almost complete removal of streptavidin tethered vesicles from the functionalized surface (Supplementary Table 1).

The concomitant change in fluorescence upon Aβ42 induced membrane permeation results in a brief lag of 8 minutes until an effect in the fluorescence signal is observed (Figure 2a, secondary y axis), which may result from the time required by the peptide to specifically adsorb to the membranes and begin to permeate the bilayers. Subsequently, there is another brief period of around 15 minutes where there is a phase of fluorescence enhancement, which is not observed with the buffer control measurement. We have previously attributed this increased fluorescence intensity as the partial dequenching of the hydrated fluorophore as it is stripped of some of the surrounding water layer as it traverses the permeated membrane channels [28]. The fluorescence intensity begins to slowly decrease after around 15 minutes as the fluorophore leaks out through the permeated membranes and continues progressively

THIS IS NOT THE VERSION OF RECORD - see doi:10.1042/BJ20110750

Accepted Manuscript

Licenced copy. Copying is not permitted, except with prior permission and as allowed by law.
© 2011 The Authors Journal compilation © 2011 Portland Press Limited

Biochemical Journal Immediate Publication. Published on 24 Jun 2011 as manuscript BJ20110750

to decrease as the dye diffuses through the permeated membranes into solution. The change in fluorescence intensity was modelled and calculated as $D^* = 3.9 \times 10^{-20}$ $m^2.sec^{-1}$. The diffusion of the dye through 0-hour incubated Aβ42 permeated membranes is around 50 times faster diffusion rate compared to the passive leakage of the dye through non-permeated control membranes (Table 2). Previously, it has been shown that Aβ40 was able to form cation-selective channels across planar lipid bilayer when the peptide was reconstituted into the lipid mixture prior to bilayer formation [36]. It was shown that preformed oligomeric Aβ reconstituted in membranes had channel activity. Complementary to this work, we suggest that Aβ42 can also cause permeation and defects within the lipid bilayer larger than discrete ion channels, capable of allowing a fluorescent dye molecule ~130kDa in size to easily pass through the permeated defects. It has also been suggested that Aβ is able to induce membrane conductance in the absence of discrete ion channel or pore formation, but was instead a result of Aβ soluble oligomers enhancing the ability of ions to move through the lipid membrane on their own [4]. Therefore, the ability of Aβ to cause membrane damage may in fact be a collection of mechanisms including channel formation, membrane thinning and/or alteration of the viscoelasticity of the bilayer membranes.

The binding data were analysed in more detail by fitting the oligomeric Aβ42-membrane response to one, two, or three exponential functions revealing that the oligomers binding to a membrane is a multivalent bi- or tri-phasic process (See Supplementary Figure 5A). Using the biphasic exponential we obtain $a_0 = 0.9081$, $a_1 = 0.0603$, $t_1 = 220$ min, $t_2 = 7$min, Chi-Square = 0.00183, correlation coefficient = 0.9963. Using the triphasic exponential, a slight improvement in the fit was observed, where $a_0 = 0.9064$, $a_1 = 0.0319$, $a_2 = 0.0269$, $a_3 = 0.0622$, $t_1 = 103$ min, $t_2 = 5$ min, $t_3 = 877$ min, Chi-Square = 0.00143, correlation coefficient = 0.9971 (supplementary table 2). However, the triphasic exponential resulted in extended time points ($t_3 = 877$ min), which is beyond the time scale of the experiment, and would result in Aβ-membrane processes that would be complicated by fibril formation at this time point. Therefore, the triphasic exponential was rejected for the purposes of our analysis. A single, monophasic 1:1 exponential resulted in a poor fit. Therefore, oligomeric Aβ-membrane interactions do not fit well and can therefore be excluded. However, the biphasic exponential modelling reveals that there are two phases of Aβ oligomer binding to phospholipid membranes, suggesting an initial phase of Aβ binding to the membranes, followed by a second phase that may be either non-specific association of the peptide to the membrane surface or self-association of the Aβ from the bulk solution to existing membrane bound Aβ resulting in amyloid assembly and the beginnings of fibrillization. From the biphasic exponential function, the $t_2 = 7$ min corresponds to the beginning of fluorescence leakage through the permeated membrane. At this time point, we have attributed this to the phase of fluorescence enhancement, where the fluorophore begins to diffuse through the

THIS IS NOT THE VERSION OF RECORD - see doi:10.1042/BJ20110750

Accepted Manuscript

Licenced copy. Copying is not permitted, except with prior permission and as allowed by law.
© 2011 The Authors Journal compilation © 2011 Portland Press Limited

Biochemical Journal Immediate Publication. Published on 24 Jun 2011 as manuscript BJ20110750

permeated membranes. The t_1 = 220 min for the biphasic exponential function corresponds with the beginning of the linear range of fluorescence diffusion, and may result from the formation of the largest defects in the bilayer membrane. Both t_1, and t_2 time phases are important points in the leakage of the fluorophore through the permeated membranes.

Monitoring the fibrillar Aβ42-Membrane Interactions by SPFS

Aβ42 fibres were prepared from stock 10 μM, 0-hour incubated Aβ42 and statically incubated for seven days and confirmed by TEM (Figure 1d), the fibres were vortexed vigorously to breakup fibrillar clusters prior to injection into the flow-cell (Figure 2b). This adsorption slowly increases until equilibrium and shows markedly different kinetics of association compared to the adsorption of 0-hour incubated Aβ42 (Figure 2a). There is no immediate sharp increase in reflectivity, which is indicative of the specific adsorption of the peptide to the membrane (as observed with 0-hour incubated Aβ42). Instead, there is a continual and gradual increase in reflectivity until equilibrium is reached at around 600 minutes. This fibrillar association suggests non-specific or weak binding between the fibres and the tethered LUVs, and if binding is mediated by the ends of the molecules, this could reflect the relatively fewer free ends compared to oligomeric species. Upon rinsing of the flow-cell with fresh HEPES pH 7.4 at 600 minutes, the weakly adsorbed Aβ42 fibres disassociate from the tethered membranes and wash off into solution. A 0.06 $ng.mm^{-2}$ increase in mass is observed, which is around ten times lower in mass adsorption compared to 0-hour incubated Aβ42. The equilibrium dissociation constant is calculated to be 8.80 x 10^{-6} M; this is a significantly lower affinity (2-fold decrease in affinity) compared to 0-hour incubated Aβ42 (Table 2). Only a K_D determination between Aβ40 and membranes has previously reported, and SPR binding of Aβ42 fibrils to lipids has not been previously studied. Using the exponential functional fit, $a_0+a_1(1\text{-}e^{-t/t1})$, fibril association with the tethered membranes is shown to fit to a single exponential function (See Supplementary Figure 5B and Supplementary table 2), a0 = 0.9473, a1 = 0.0567, t1 = 245 min, Chi-Square = 0.00149, correlation coefficient = 0.9967. Addition of a second fit did not improve the fit, suggesting that fibril binding to the membrane occurs in a monophasic 1:1 binding model, which is significantly different compared to the biphasic process associated with oligomeric Aβ42 interactions with the membrane.

The change in fluorescence upon fibrillar permeation of the LUVs results in a brief five-minute period of fluorescence enhancement, similar to that observed with the addition of 0-hour incubated oligomeric Aβ42. The fluorescence intensity begins to slowly decrease after around five minutes as the fluorophore leaks out through the permeated membranes. The fluorophore leakage progressively decreases as the dye diffuses through the permeated membranes into solution. The calculated apparent dye diffusion coefficient of D^* = 3.65 x

THIS IS NOT THE VERSION OF RECORD - see doi:10.1042/BJ20110750

Accepted Manuscript

Licenced copy. Copying is not permitted, except with prior permission and as allowed by law.
© 2011 The Authors Journal compilation © 2011 Portland Press Limited

Biochemical Journal Immediate Publication. Published on 24 Jun 2011 as manuscript BJ20110750

10^{-22} $m^2.sec^{-1}$ is not significantly different compared to the passive leakage of the dye through non-permeated control membranes, and results in significantly less leakage (1.96-fold decrease) compared to oligomeric Aβ42 induced membrane permeation (Table 2). Although the overall decrease in normalized fluorescence may appear to be similar between fibres and oligomers, it is not relevant to compare these decrease in fluorescence values and encapsulation efficiencies and LUV capturing may and do vary from experiment to experiment, so they can not be directly compared. The only true means of comparing the permeation is by comparing the apparent dye diffusion coefficients. We have calculated a D* value of 3.9 x 10^{-20} $m^2.sec^{-1}$ from Aβ oligomers compared to $D^* = 3.65 \times 10^{-22}$ $m^2.sec^{-1}$ for fibrils. Our results, showing that 0-hour Aβ binds and causes permeation of LUVs more strongly than fibrillar Aβ, suggest that binding to the membrane and subsequent elongation are linked to the resulting membrane damage leading to permeation.

GM1 Influences both Oligomeric Aβ42-Membrane Binding and Permeation

Monitoring the Oligomeric Aβ42-GM1 Deficient Membrane Interactions by SPFS

The GM1-ganglioside expression in biological membranes has been reported to affect the interactions between the Aβ peptide and the membranes, and in our previous work we have shown that the removal of GM1 from the composition of the membranes results in greater than 50 % decrease in permeation of membranes [12]. In this study we examined the effect of the GM1 within the tethered membrane vesicles, in simultaneously modulating the binding and permeation of 0-hour incubated Aβ42. The addition of 10 μM 0-hour incubated Aβ42 to tethered LUVs without GM1 (see table 1 for LUV composition) causes an immediate increase in reflectivity as the Aβ42 binds to the membranes within the initial 20 minutes (Figure 2c). The preliminary binding kinetics appears to be slower compared to when GM1 is present, and the initial binding kinetics are around three times slower to reach initial equilibrium compared to when GM1 is present in the bilayers (Figure 2a). The adsorption of the Aβ42 to the membranes not containing GM1 then follows a slower phase of binding until equilibrium is reached around 900 minutes after Aβ42 injection. Upon reaching equilibrium, there is a small decrease in reflectivity, which may be the result of partial loss of non-specifically adsorbed peptide from the tethered LUVs. There is a 0.19 $ng.mm^{-2}$ increase in mass at the supported surface, which is around three times less than when GM1 is present. The equilibrium dissociation constant is calculated to be 8.90 x 10^{-7} M, this is an approximately 1.8-fold lower binding affinity compared to when GM1 is present (Table 2). From the binding kinetics, it suggests that GM1 is involved in modulating Aβ42 oligomer binding, and its exclusion from the membranes decreases the binding affinity. Binding of the oligomeric peptide to the tethered membranes is still observed, suggesting that Aβ also can bind to other components found within our LUVs, such as cholesterol and/or the phospholipids.

THIS IS NOT THE VERSION OF RECORD - see doi:10.1042/BJ20110750

Accepted Manuscript

Licenced copy. Copying is not permitted, except with prior permission and as allowed by law.
© 2011 The Authors Journal compilation © 2011 Portland Press Limited

Biochemical Journal Immediate Publication. Published on 24 Jun 2011 as manuscript BJ20110750

The binding of Aβ peptide to GM1 appears to be concentration dependent, and with increasing GM1 concentration there is an increase of Aβ42 binding. The addition of 10 μM 0-hour incubated Aβ42 to tethered LUVs containing varying physiologically relevant proportions of GM1 (0, 2, 5,10, and 15 mole %) causes varying increases in reflectivity and minima shifts, which were plotted against GM1 concentration (Figure 3). From this plot the R_{eq} is determined as 1 mole %. Above 5 mole % GM1 the Aβ42 binding becomes saturated and equilibrium is reached, whereby no further increase in Aβ42 binding is observed. Ensuring that the GM1 molar fraction is between the R_{eq} and R_{max} ensures maximal binding efficiency without saturating the LUV membranes.

SPFS for tethered vesicles without GM1 show very little change in fluorescence on addition of Aβ oligomers (Figure 2c), and the fluorophore leakage shows similar kinetics to the buffer control experiment. The change in fluorescence intensity is calculated as $D^* = 1.41 \times 10^{-22}$ $m^2.sec^{-1}$, and is significantly different (1.99-fold decrease) compared to the oligomeric permeation of membranes (Table 2). The decrease in fluorescence leakage observed when no GM1 is present, suggests that the GM1 may play a role in modulating Aβ permeation.

The removal of the GM1 gangliosides from the membrane composition has been reported to potentially destabilize membranes [37] therefore in our experiments we would theoretically observe a potentially greater Aβ-induced membrane permeation. However, the decrease in D^* and lower apparent dye diffusion observed between Aβ and membranes not containing GM1 is probably the result of GM1 modulating Aβ-membrane binding and not a result of altered membrane stability. The increased binding observed between Aβ and GM1-containing membranes may be the result of gangliosides ability to form clusters, which are able to interact with various membrane components and membrane proteins [38], thereby increasing the local concentration of bound Aβ peptides on the membrane and increasing the potential for Aβ-Aβ interactions. This is supported by previous studies that have suggested a role for GM1 in seeding aggregation of Aβ [39]. The influence of electrostatic interactions is believed to play a key role in modulating Aβ-GM1 interactions, as at pH 5.5 Aβ40 is slightly positively charged and the headgroup of GM1 is negatively charged, whereby the peptide shows greater insertion pressure compared to when Aβ40 inserts into GM1-containing membranes at pH 7.2 where Aβ is negatively charged [14].

Observation of Aβ42-Membrane Interactions by Atomic Force Microscopy

In order to directly visualize the association and effect of oligomeric or fibrillar Aβ on membranes, we have used atomic force microscopy (AFM) allowing the monitoring of elongation and permeation. AFM images reveal heights of the sample above the surface

THIS IS NOT THE VERSION OF RECORD - see doi:10.1042/BJ20110750

Accepted Manuscript

Licenced copy. Copying is not permitted, except with prior permission and as allowed by law.
© 2011 The Authors Journal compilation © 2011 Portland Press Limited

Biochemical Journal Immediate Publication. Published on 24 Jun 2011 as manuscript BJ20110750

whereby associations with the bilayer will appear light and holes or defects appear dark. A freshly prepared mica supported bilayer was scanned in tapping mode AFM (Figure 4a) prior to the addition of the Aβ42 to ensure complete bilayer formation and for comparison to Aβ adsorbed bilayers. Injection of 10 μM 0-hour incubated Aβ42 shows the association of the peptide to the membranes (Figure 4b). A variety of morphological oligomeric Aβ42 species is observed on the membrane surface. An aliquot of the Aβ42 injected into the AFM flow-cell was used to prepare a transmission electron micrograph for comparison (Figure 4f). The TEM shows similar morphological peptide species to that observed on the membrane via AFM, which include circular oligomers ranging between 20-50 nm in diameter, and curvilinear oligomers that are 70-85 nm in length. AFM images were scanned in tapping mode upon incubation of the 0-hour incubated Aβ42 with the bilayers over an hour time course to visualize the changes in peptide and bilayer (Figure 4b-e). Deposition of Aβ42 onto the membrane surface occurs immediately following injection, with a visible roughening of the smooth membrane surface. Increasing amounts of Aβ42 assemblies are observed during the incubation of the peptide with the bilayer, which include a great abundance of circular oligomers, and the emergence of a few short fibrillar species (Figure 4c). After further incubation, an increasing number of small circular oligomers, protofibrils, and a small number of short fibrils are observed (Figure 4e). After incubating the peptide and bilayers for 1 hour a greater abundance of 200 nm protofibrils appear adsorbed to the membrane and much longer 600-1000 nm fibres. The assembly of Aβ42 oligomers into fibres can clearly be visualized by AFM (Figure 4g-i and j-k), and structures looking like ‘strings of beads’ can be seen to begin to form fibres.

The adsorption of the peptide to the bilayer causes the appearance of defects in the bilayer structure, as the membrane changes from an apparently smooth structure with a few discrete double bilayer patches and defects revealing the mica substrate 5 nm below (Figure 4a), to a rough bilayer as the Aβ adsorbs (Figure 4b-e). Small irregular imperfections and indentations ranging 10-100 nm begin to emerge within 30 seconds of the Aβ42 adsorbing to the membrane surface (Figure 4b), and these ill-defined defects appear to only permeate through the first lipid monolayer of the bilayer membranes. A cross section plot shows a depth of around 3-4 nm (Figure 5a). Upon further incubation of the Aβ42 with the bilayers, these defects become obvious holes with well-defined circular edges peppered across the entire bilayer surface, these holes range between 10-100 nm in diameter (Figure 4d), and appear to permeate through both leaflets of the bilayer membrane. From profile scans the holes were calculated to be 6.2 $\pm$ 0.2nm deep(Figure 5b). The depth of the holes is slightly deeper than the unpermeated membrane (5nm) before Aβ addition, which could either result from the adsorption of the peptide to the bilayer or as a result of the Aβ causing the acyl chains of the phospholipids to swell and change the fluidity of the membranes [23]. During the one-hour

THIS IS NOT THE VERSION OF RECORD - see doi:10.1042/BJ20110750

Accepted Manuscript

Licenced copy. Copying is not permitted, except with prior permission and as allowed by law.
© 2011 The Authors Journal compilation © 2011 Portland Press Limited

Biochemical Journal Immediate Publication. Published on 24 Jun 2011 as manuscript BJ20110750

time course of Aβ42-bilayer incubation the regions of permeation tend to vary in diameter and the defects within the membrane are seen to range from a few nanometres up to large areas of permeation up to 280 nm in diameter where several defects merge to form larger holes. 5.4% ± 0.8% (standard deviation 1.8%) loss of bilayer by Aβ42 permeation resulted, suggesting that Aβ may act by a combination of both pore formation and detergent-like fashion causing the removal of lipids from the bilayer surface and therefore altering the viscoelasticity of the membrane. AFM therefore, gave us a direct means to visualize the adsorption of the Aβ42 in the presence of bilayer membrane, but also showed the permeation of these membranes, initially forming defects which did not permeate the membrane fully (Figure 5a), but during the incubation these defects became holes that permeated all the way through the bilayer (Figure 5b). Imaging of the bilayer with the lightest force show quite large quantities of loosely bound peptide together with patches of ejected bilayer floating on top. More than a single image of the same area resulted in the holes refilling with bilayer, a process driven by the scanning AFM probe. A zoom out following an initial scan reveals holes on the unscanned perimeter, with a fully smooth square with closed-up holes from the previous scan (data not shown). The refilled holes were obvious as fresh bilayer with little adsorbed peptide (Figure 4g-i and j-k). To avoid this AFM driven healing effect, the scan area was changed each time with a manual translation. The holes, once formed, appear stable over time. Bilayer is ejected from the surface as the holes appear, and as the bilayer is solid supported there is no excess lateral pressure to drive the holes to close up. Conversely, in a vesicle, or real cell membrane, the flexible membrane could change shape and size to some degree, minimising or even closing up the hole. Therefore the hole is less transient and possibly much larger. Similar effects have been previously observed for amylin association with lipid bilayer at lower magnification by confocal microscopy, showing immediate defects in the membrane following administration of oligomeric amylin [40]. The authors suggest a direct and strong interaction between the fibrillising peptide and the lipid molecules.

In contrast to the dramatic effect of oligomeric Aβ42 on lipid bilayers, the addition of 10 μmol.dm^{-3} fibrillar Aβ42 to the bilayer surface resulted in no apparent fibrillar association with the membranes and despite fibrils being observed for the samples by electron microscopy, no fibrils were observed by AFM and no images could be obtained. This may have resulted from the weak association of the fibrillar peptide being swept away by the AFM probe during imaging, even when using the lightest force. This supports the SPFS results showing that fibrillar binding to membranes is non-specific, and weakly bound peptide does not have high affinity for the biomimetic membranes. In contrast, fibres that had been grown from 0-hour incubated Aβ42 in the *presence* of the bilayer remained strongly adhered and could be imaged by AFM (Figure 4).

THIS IS NOT THE VERSION OF RECORD - see doi:10.1042/BJ20110750

Accepted Manuscript

Licenced copy. Copying is not permitted, except with prior permission and as allowed by law.
© 2011 The Authors Journal compilation © 2011 Portland Press Limited

Biochemical Journal Immediate Publication. Published on 24 Jun 2011 as manuscript BJ20110750

Three structurally divergent models for Aβ-membrane permeation have been proposed; i) carpeting of the peptide on one leaflet of the membrane surface, which results in an asymmetric pressure between the two leaflets [41]; ii) The formation of stable pores and ion channels has been proposed for amyloid induced toxicity, whereby the disruption of Ca^{2+} homeostasis has been observed as a potential mechanism associated with AD; iii) Detergent-like effects of amyloid-induced membrane damage are believed to occur through the association of the amyloid peptides in the form of micelle-like structures with the membrane surface. At high local peptide concentrations on the membrane surface, either after the surface is covered with peptide monomers or oligomers or through the association between membrane-bound amyloid a detergent effect is observed [42].

Atomic force microscopy has previously shown apparent channel formation by Aβ42 that had been reconstituted into liposomes [43]. In contrast, here we show that Aβ42 administered to the lipid bilayer causes immediate defects upon binding. This result is also in contrast to a study showing that TFA solubilized Aβ42 association with total brain extract bilayers assembled to form fibrils with no apparent damage to the membrane [7]. However, advances in Aβ42 peptide preparation and formation of oligomers may be responsible for these differences. In our work, the Aβ42 has been solubilized using newly established methods to ensure disaggregation and also removal of all solvents [12]. The AFM studies reveal almost immediate and dramatic changes to the lipid bilayer in response to binding of Aβ42 and its assembly on the membrane, showing for the first time the changes associated with membrane permeation of oligomeric Aβ42.

Conclusions

The assembly of Aβ42 has been implicated in the cytotoxicity effects, and has been reported to be associated with early oligomeric amyloid species. The oligomeric Aβ affects the integrity of the membrane structure, and may also provide a route for the uptake of the Aβ into the cytosolic environment of the cells or affect internal organelles (please see accompanying paper). Here we have shown that 0-hour incubated Aβ42 oligomers bind with greater affinity and cause greater permeation to synthetic membranes compared to fibrillar Aβ42. Oligomeric Aβ42 binding appears to follow a biphasic interaction with the membrane, whereby there is an initial phase of specific adsorption, followed by a secondary phase of either non-specific association of the peptide with the membrane or the self-association of the peptide as it assembles and fibrillizes. Moreover, the association of fibrillar Aβ42 with membranes follows a monophasic exponential fitting. We postulate that this assembly from oligomer to fibrils, may cause some mechanical defects in the membranes. The SPFS methods have allowed us to directly correlate the binding with the permeation of the lipid vesicles. The GM1-ganglioside appears to affect the binding of the oligomeric peptide to the

THIS IS NOT THE VERSION OF RECORD - see doi:10.1042/BJ20110750

Accepted Manuscript

Licenced copy. Copying is not permitted, except with prior permission and as allowed by law.
© 2011 The Authors Journal compilation © 2011 Portland Press Limited

Biochemical Journal Immediate Publication. Published on 24 Jun 2011 as manuscript BJ20110750

membrane surface and also modulates the permeation, whereby the exclusion of GM1 from the membrane composition results in decreased Aβ42 binding and decreased permeation. It has been previously suggested that GM1 may form microdomains that seed association and aggregation of Aβ42 [44]. Direct visualization of the permeation of the membranes by AFM reveals initial defects where the peptide begins to penetrate the upper monolayer of the bilayers that develop with time to become discrete holes up to 200 nm in diameter. This membrane damage appears to be directly correlated with growth of the peptide to form fibrillar deposits on the membrane. From these unique findings in our study of Aβ-directed membrane permeation, we suggest that soluble oligomeric Aβ may possess several mechanisms of inducing cell death, and the formation of holes in the membrane and altered viscoelasticity of the membrane may be crucial in modulating cell toxicity. Taken together our results reveal a direct correlation between binding and assembly of Aβ42 on the membrane with the observed leakage from vesicles and holes forming in lipid bilayers. These observations have important implications for the cytotoxic activity of the Aβ42 oligomers relevant to Alzheimer's disease pathology.

Acknowledgements

The authors would like to thank Dr Julian Thorpe for all his help and guidance with electron microscopy. We thank Professor Stephen Evans (Leeds) for his guidance and support. We are grateful for the generous researcher exchange prize given by the Synthetic Components Network, and the Leeds EPSRC Nanoscience and Nanotechnology Research Equipment Facility (LENNF). We would also like to thank Dr Petra Cameron and Eleanor Johnson from the University of Bath for help and advice with the SPFS.

Funding

TLW and LCS are supported by Alzheimer's research UK (previously Alzheimer's Research Trust), and BU is supported by the National Institute of Health A6027818 grant, and we are sincerely grateful for their funding.

THIS IS NOT THE VERSION OF RECORD - see doi:10.1042/BJ20110750

Accepted Manuscript

Licenced copy. Copying is not permitted, except with prior permission and as allowed by law.
© 2011 The Authors Journal compilation © 2011 Portland Press Limited

Biochemical Journal Immediate Publication. Published on 24 Jun 2011 as manuscript BJ20110750

Figure legends

Figure 1. Scanning and Transmission Electron Micrographs of Tethered LUVs and Time Course of Negatively Stained Aβ42 assembly respectively. (a) SEM of Tethered LUVs. Time course shows the results of 100 μM Aβ42 assembled *in vitro* after incubation for time periods of; (b) 0 hours, (c) 20 hours, (d) Aβ42 fibres for SPFS-membrane interaction study.

Figure 2. SPR and SPFS Measurement of Oligomeric Aβ42, Fibrillar Aβ42, GM1-Aβ42 Association and Permeation of LUVs. Tethered LUVs and Aβ interactions observed as change in reflected light intensity (Reflectivity —, primary y-axis) and dye diffusion of the Alexa Fluor 647 from the LUV aqueous space into the external surrounding medium (Fluorescence **.....**, secondary y-axis). (a) 10 μM 0-hour incubated Aβ42 was added to tethered LUVs and monitored the specific binding of the peptide to the membranes by SPR, and the associated permeation of the membranes by SPFS as changes in fluorescence. (b). 10 μM 168-hour incubated (fibrillar) Aβ42 was added to tethered LUVs and monitored the binding of the fibrils to the membranes by SPR, and the associated permeation of the membranes by SPFS as changes in fluorescence. (c) 10 μM 0-hour incubated Aβ42 was added to tethered GM1-deficient LUVs and monitored the binding of the oligomeric peptide to the membranes by SPR, and the associated permeation of the membranes by SPFS as changes in fluorescence.

Figure 3. Equilibrium Response, R_{eq}, Determination from GM1 Concentration Vs Reflectivity Change using the Langmuir Equation. 10μmol.dm^{-3} Aβ42 time = 0 hours was added to LUVs containing 0, 2, 5, 10, and 15 molar % of GM1, and the change in mass density monitored. The change in adsorbed mass was plotted against GM1 concentration.

Figure 4. Atomic Force Micrographs of the Interaction Between Aβ42 Oligomers and Membrane Bilayers. (a) AFM image of 5 x 5 μm planar lipid bilayer, with small patches of secondary bilayer (lighter, circular patches) and defects (black patches) observed (b) 10 μM 0-hour incubated Aβ42 was added to mica supported bilayers 5 x 5 μm, small oligomeric Aβ42 is observed on the bilayer surface. (c-d) Successive AFM images of 10 μM 0-hour incubated Aβ42 over and hour time course showing fibrillization of Aβ42. (e) AFM images of 10 x 10 μm lipid bilayer and the adsorbed 10 μM 0-hour incubated Aβ42 after 1 hour incubation. Small and large defects and holes (up to 100nm in diameter) appear peppered within the lipid bilayer as a result of Aβ42 induced membrane permeation, (f) TEM image of the 0-hour incubated Aβ42 taken at same time as injection of the peptide in the AFM of 4b, showing similar morphologies of the peptide for comparison. (g-k) Digital zooms to 1.5μm

THIS IS NOT THE VERSION OF RECORD - see doi:10.1042/BJ20110750

Accepted Manuscript

Licenced copy. Copying is not permitted, except with prior permission and as allowed by law.
© 2011 The Authors Journal compilation © 2011 Portland Press Limited

Biochemical Journal Immediate Publication. Published on 24 Jun 2011 as manuscript BJ20110750

from 10 x 10 μm scans of 10 μM 0-hour incubated Aβ42 over a 1 hour time course, the three (g-i) and two (j-k) successive images fibrillization of the peptide on the bilayer surface.

Figure 5. Atomic Force Micrograph Profile of the Permeation Holes Due to the Interaction Between Aβ42 Oligomers and Membrane Bilayers. AFM image of 2 x 2 μm planar lipid bilayer, with profile cross sectional analysis. a) Immediately following addition of Aβ revealing depths of defects/holes of 3-4 nm, b) following incubation of Aβ on the membrane showing depths of 6.2 ± 0.2 nm. Red arrows show corresponding regions of the image and cross-sectional plot.

THIS IS NOT THE VERSION OF RECORD - see doi:10.1042/BJ20110750

Accepted Manuscript

Licenced copy. Copying is not permitted, except with prior permission and as allowed by law.
© 2011 The Authors Journal compilation © 2011 Portland Press Limited

Biochemical Journal Immediate Publication. Published on 24 Jun 2011 as manuscript BJ20110750

THIS IS NOT THE VERSION OF RECORD - see doi:10.1042/BJ20110750

Accepted Manuscript

Licenced copy. Copying is not permitted, except with prior permission and as allowed by law.
© 2011 The Authors Journal compilation © 2011 Portland Press Limited

Biochemical Journal Immediate Publication. Published on 24 Jun 2011 as manuscript BJ20110750

THIS IS NOT THE VERSION OF RECORD - see doi:10.1042/BJ20110750

Accepted Manuscript

References

1 Kukar, T. L., Ladd, T. B., Bann, M. A., Fraering, P. C., Narlawar, R., Maharvi, G. M., Healy, B., Chapman, R., Welzel, A. T., Price, R. W., Moore, B., Rangachari, V., Cusack, B., Eriksen, J., Jansen-West, K., Verbeeck, C., Yager, D., Eckman, C., Ye, W., Sagi, S., Cottrell, B. A., Torpey, J., Rosenberry, T. L., Fauq, A., Wolfe, M. S., Schmidt, B., Walsh, D. M., Koo, E. H. and Golde, T. E. (2008) Substrate-targeting gamma-secretase modulators. Nature. **453**, 925-929

2 Glenner, G. G. and Wong, C. W. (1984) Alzheimer's disease: initial report of the purification and characterization of a novel cerebrovascular amyloid protein. Biochem. Biophys. Res. Commun. **120**, 885-890

3 Citron, M., Westaway, D., Xia, W., Carlson, G., Diehl, T., Levesque, G., Johnson-Wood, K., Lee, M., Seubert, P., Davis, A., Kholodenko, D., Motter, R., Sherrington, R., Perry, B., Yao, H., Strome, R., Lieberburg, I., Rommens, J., Kim, S., Schenk, D., Fraser, P., St George Hyslop, P. and Selkoe, D. J. (1997) Mutant presenilins of Alzheimer's disease increase production of 42-residue amyloid beta-protein in both transfected cells and transgenic mice. Nature Medicine. **3**, 67-72

4 Kayed, R., Sokolov, Y., Edmonds, B., McIntire, T. M., Milton, S. C., Hall, J. E. and Glabe, C. G. (2004) Permeablization of lipid bilayers is a common conformation-dependent activity of soluble oligomers in protein misfolding diseases. J. Biol. Chem. **279**, 46363-46366

5 Kremer, J. J., Sklansky, D. J. and Murphy, R. M. (2001) Profile of changes in lipid bilayer structure caused by beta-amyloid peptide. Biochemistry. **40**, 8563-8571

6 Subasinghe, S., Unabia, S., Barrow, C. J., Mok, S. S., Aguilar, M. I. and Small, D. H. (2003) Cholesterol is necessary both for the toxic effect of Abeta peptides on vascular smooth muscle cells and for Abeta binding to vascular smooth muscle cell membranes. J. Neurochem. **84**, 471-479

7 Yip, C. M., Darabie, A. A. and McLaurin, J. (2002) Abeta42-peptide assembly on lipid bilayers. J. Mol. Biol. **318**, 97-107

8 McLaurin, J. and Chakrabartty, A. (1996) Membrane disruption by Alzheimer's b-amyloid peptides mediated by specific binding to either phospholipids of gangliosides: implications for neurotoxicity. J. Biol. Chem. **271**, 26482-26489

9 Arispe, N., Pollard, H. B. and Rojas, E. (1993) Giant multilevel cation channels formed by Alzheimer disease amyloid beta-protein [A beta P-(1-40)] in bilayer membranes. Proceedings of the National Academy of Sciences of the United States of America. **90**, 10573-10577

10 Bitan, G., Fradinger, E. A., Spring, S. M. and Teplow, D. B. (2005) Neurotoxic protein oligomers--what you see is not always what you get. Amyloid. **12**, 88-95

11 Fezoui, Y., Hartley, D. M., Harper, J. D., Khurana, R., Walsh, D. M., Condron, M. M., Selkoe, D. J., Lansbury, P. T., Jr., Fink, A. L. and Teplow, D. B. (2000) An improved

Licenced copy. Copying is not permitted, except with prior permission and as allowed by law.
© 2011 The Authors Journal compilation © 2011 Portland Press Limited

Biochemical Journal Immediate Publication. Published on 24 Jun 2011 as manuscript BJ20110750

method of preparing the amyloid beta-protein for fibrillogenesis and neurotoxicity experiments. Amyloid. **7**, 166-178

12 Williams, T. L., Day, I. J. and Serpell, L. C. (2010) The effect of Alzheimer's abeta aggregation state on the permeation of biomimetic lipid vesicles. Langmuir. **26**, 17260-17268

13 Ashley, R. H., Harroun, T. A., Hauss, T., Breen, K. C. and Bradshaw, J. P. (2006) Autoinsertion of soluble oligomers of Alzheimer's Abeta(1-42) peptide into cholesterol-containing membranes is accompanied by relocation of the sterol towards the bilayer surface. BMC Struct. Biol. **6**, 21

14 Chi, E. Y., Frey, S. L. and Lee, K. Y. (2007) Ganglioside G(M1)-mediated amyloid-beta fibrillogenesis and membrane disruption. Biochemistry. **46**, 1913-1924

15 Choo-Smith, L. P. and Surewicz, W. K. (1997) The interaction between Alzheimer amyloid beta(1-40) peptide and ganglioside GM1-containing membranes. FEBS letters. **402**, 95-98

16 Valdes-Gonzalez, T., Inagawa, J. and Ido, T. (2001) Neuropeptides interact with glycolipid receptors: a surface plasmon resonance study. Peptides. **22**, 1099-1106

17 Sonnino, S., Mauri, L., Chigorno, V. and Prinetti, A. (2007) Gangliosides as components of lipid membrane domains. Glycobiology. **17**, 1R-13R

18 Weng, K. C., Kanter, J. L., Robinson, W. H. and Frank, C. W. (2006) Fluid supported lipid bilayers containing monosialoganglioside GM1: a QCM-D and FRAP study. Colloids Surf. B Biointerfaces. **50**, 76-84

19 Yokoyama, S., Takeda, T. and Abe, M. (2001) Inhibition effects of gangliosides G(M1), G(D1a) and G(T1b) on base-catalyzed isomerization of prostaglandin A(2). Colloids Surf. B Biointerfaces. **20**, 361-368

20 Yokoyama, S., Ohta, Y., Sakai, H. and Abe, M. (2004) Effect of membrane composition on surface states of ganglioside GM1/dipalmitoylphosphatidylcholine/dioleoylphosphatidylcholine monolayers. Colloids Surf. B Biointerfaces. **34**, 65-68

21 Mikhalyov, I., Olofsson, A., Grobner, G. and Johansson, L. B. (2010) Designed fluorescent probes reveal interactions between amyloid-beta(1-40) peptides and GM1 gangliosides in micelles and lipid vesicles. Biophys. J. **99**, 1510-1519

22 Zhiyou, C., Yong, Y., Shanquan, S., Jun, Z., Liangguo, H., Ling, Y. and Jieying, L. (2009) Upregulation of BACE1 and beta-amyloid protein mediated by chronic cerebral hypoperfusion contributes to cognitive impairment and pathogenesis of Alzheimer's disease. Neurochem. Res. **34**, 1226-1235

23 Muller, W. E., Kirsch, C. and Eckert, G. P. (2001) Membrane-disordering effects of beta-amyloid peptides. Biochemical Society transactions. **29**, 617-623

THIS IS NOT THE VERSION OF RECORD - see doi:10.1042/BJ20110750

Accepted Manuscript

Licenced copy. Copying is not permitted, except with prior permission and as allowed by law.
© 2011 The Authors Journal compilation © 2011 Portland Press Limited

Biochemical Journal Immediate Publication. Published on 24 Jun 2011 as manuscript BJ20110750

24 Ying, N., BaiYang, S., Bo, S., LingLing, L., Zhang, Z. and Zhao, N. (2009) Endogenously generated amyloid β|increases mem-brane fluidity in neural 2a cells. Chinese Science Bulletin. **54**, 394-398

25 Engel, M. F., Khemtemourian, L., Kleijer, C. C., Meeldijk, H. J., Jacobs, J., Verkleij, A. J., de Kruijff, B., Killian, J. A. and Hoppener, J. W. (2008) Membrane damage by human islet amyloid polypeptide through fibril growth at the membrane. Proceedings of the National Academy of Sciences of the United States of America. **105**, 6033-6038

26 Khemtemourian, L., Killian, J. A., Hoppener, J. W. and Engel, M. F. (2008) Recent insights in islet amyloid polypeptide-induced membrane disruption and its role in beta-cell death in type 2 diabetes mellitus. Experimental diabetes research. **2008**, 421287

27 Williams, T. L., Vareiro, M. M. and Jenkins, A. T. (2006) Fluorophore-encapsulated solid-supported bilayer vesicles: a method for studying membrane permeation processes. Langmuir. **22**, 6473-6476

28 Williams, T. L. and Jenkins, A. T. (2008) Measurement of the binding of cholera toxin to GM1 gangliosides on solid supported lipid bilayer vesicles and inhibition by europium (III) chloride. J. Am. Chem. Soc. **130**, 6438-6443

29 Capone, R., Quiroz, F. G., Prangkio, P., Saluja, I., Sauer, A. M., Bautista, M. R., Turner, R. S., Yang, J. and Mayer, M. (2009) Amyloid-beta-induced ion flux in artificial lipid bilayers and neuronal cells: resolving a controversy. Neurotox. Res. **16**, 1-13

30 Nichols, M. R., Moss, M. A., Reed, D. K., Hoh, J. H. and Rosenberry, T. L. (2005) Amyloid-beta aggregates formed at polar-nonpolar interfaces differ from amyloid-beta protofibrils produced in aqueous buffers. Microsc. Res. Tech. **67**, 164-174

31 Hirota-Nakaoka, N., Hasegawa, K., Naiki, H. and Goto, Y. (2003) Dissolution of beta-2 microglobulin amyloid fibrils by dimethylsulfoxide. J Biochem (Japan). **134**, 159-164

32 Booth, C., Bushby, R. J., Cheng, Y. L., Evans, S. D., Liu, Q. Y. and Zhang, H. L. (2001) Synthesis of novel biotin anchors. Tetrahedron. **57**, 9859-9866

33 Yu, F., Persson, B., Lofas, S. and Knoll, W. (2004) Attomolar sensitivity in bioassays based on surface plasmon fluorescence spectroscopy. J. Am. Chem. Soc. **126**, 8902-8903

34 Liebermann, T. and Knoll, W. (2003) Parallel Multispot Detection of Target Hybridization to Surface-Bound Probe Oligonucleotides of Different Base Mismatch by Surface-Plasmon Field-Enhanced Fluorescence Microscop. Langmuir. **19**, 1567-1572

35 Abramoff, M. D., Magelhaes, P. J. and Ram, S. J. (2004) Image Processing with ImageJ. Biophotonics International. **11**, 36-42

36 Arispe, N., Rojas, E. and Pollard, H. (1993) Alzheimer's disease amyloid b protein forms calcium channels in bilayer membranes: Blockade by tromethamine and aluminium. Proc. Natl. Acad. Sci. USA. **90**, 567-571

THIS IS NOT THE VERSION OF RECORD - see doi:10.1042/BJ20110750

Accepted Manuscript

Licenced copy. Copying is not permitted, except with prior permission and as allowed by law.
© 2011 The Authors Journal compilation © 2011 Portland Press Limited

Biochemical Journal Immediate Publication. Published on 24 Jun 2011 as manuscript BJ20110750

37 Lin, M.-S. (2007) Kinetics and enthalpy measurements of interaction between β-amyloid and liposomes by surface plasmon resonance and isothermal titration microcalorimetry. Colloids and Surfaces B: Biointerfaces. **58**, 231

38 Todeschini, A. R., Dos Santos, J. N., Handa, K. and Hakomori, S. I. (2008) Ganglioside GM2/GM3 complex affixed on silica nanospheres strongly inhibits cell motility through CD82/cMet-mediated pathway. Proceedings of the National Academy of Sciences of the United States of America. **105**, 1925-1930

39 Choo-Smith, L. P., Garzon-Rodriguez, W., Glabe, C. G. and Surewicz, W. K. (1997) Acceleration of amyloid fibril formation by specific binding of Abeta-(1-40) peptide to ganglioside-containing membrane vesicles. The Journal of biological chemistry. **272**, 22987-22990

40 Domanov, Y. A. and Kinnunen, P. K. (2008) Islet amyloid polypeptide forms rigid lipid-protein amyloid fibrils on supported phospholipid bilayers. J Mol. Biol. **376**, 42-54

41 Hebda, J. A. and Miranker, A. D. (2009) The interplay of catalysis and toxicity by amyloid intermediates on lipid bilayers: insights from type II diabetes. Annual review of biophysics. **38**, 125-152

42 Shai, Y. (1999) Mechanism of the binding, insertion and destabilization of phospholipid bilayer membranes by alpha-helical antimicrobial and cell non-selective membrane-lytic peptides. Biochim. Biophys. Acta. **1462**, 55-70

43 Lin, H., Bhatia, R. and Lal, R. (2001) Amyloid beta protein forms ion channels: implications for Alzheimer's disease pathophysiology. Faseb J. **15**, 2433-2444

44 Matsuzaki, K., Kato, K. and Yanagisawa, K. (2010) Abeta polymerization through interaction with membrane gangliosides. Biochim. Biophys. Acta. **1801**, 868-877

THIS IS NOT THE VERSION OF RECORD - see doi:10.1042/BJ20110750

Accepted Manuscript

Licenced copy. Copying is not permitted, except with prior permission and as allowed by law.
© 2011 The Authors Journal compilation © 2011 Portland Press Limited

Biochemical Journal Immediate Publication. Published on 24 Jun 2011 as manuscript BJ20110750

Table 1. Bilayer Composition Summary. Percentage composition of the tethered LUVs containing and excluding GM1 and encapsulating Alexa Fluor 647 water soluble dye, and the composition of mica supported bilayers for AFM.

Membrane component	SPFS LUVs (%)	SPFS GM1-deficient LUVs (%)	AFM bilayers (%)
DMPC	50.2	51.75	51
DMPE	13.4	13.8	13.6
DMPG	1.7	1.725	1.7
DMPS	1.7	1.725	1.7
Cholesterol	30	30	30
GM1	2	-	2
Biotin-PE	1	1	-
Alexa Fluor ^{647}	5μM	5μM	-
Final Lipid Concentration	0.5 mg.mL^{-1}	0.5 mg.mL^{-1}	1 mg.mL^{-1}

THIS IS NOT THE VERSION OF RECORD - see doi:10.1042/BJ20110750

Accepted Manuscript

Licenced copy. Copying is not permitted, except with prior permission and as allowed by law.
© 2011 The Authors Journal compilation © 2011 Portland Press Limited

Biochemical Journal Immediate Publication. Published on 24 Jun 2011 as manuscript BJ20110750

Table 2. Comparison of the Equilibrium Dissociation Constants (K_D) and Apparent Dye Diffusion Coefficient (D*) between Oligomeric Aβ42 and Fibrillar Aβ42 with GM1-containing and GM1-deficient Membranes.

Peptide-Membrane Interaction System	**Equilibrium dissociation constant, K_D, (mol.dm^{-3})**	**Apparent Dye Diffusion Coefficient, D*, (m^2.sec^{-1})**
Control	0	7.29×10^{-22}
Oligomeric Aβ42-Membrane	2.68×10^{-8}	3.9×10^{-20}
Fibrillar Aβ42-Membrane	8.80×10^{-6}	3.65×10^{-22}
Aβ42-GM1 deficient Membrane	8.90×10^{-7}	1.41×10^{-22}

THIS IS NOT THE VERSION OF RECORD - see doi:10.1042/BJ20110750

Accepted Manuscript

Licenced copy. Copying is not permitted, except with prior permission and as allowed by law.
© 2011 The Authors Journal compilation © 2011 Portland Press Limited

Biochemical Journal Immediate Publication. Published on 24 Jun 2011 as manuscript BJ20110750

THIS IS NOT THE VERSION OF RECORD - see doi:10.1042/BJ2011

Figure 1.

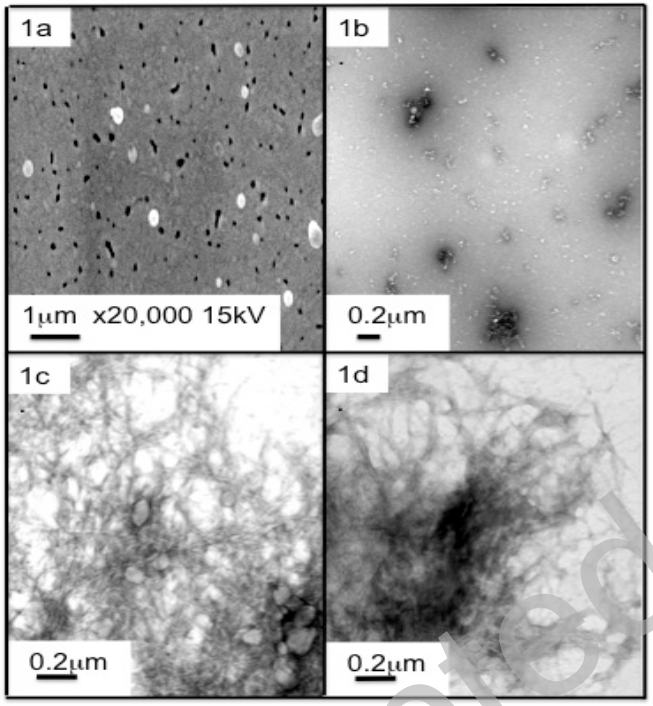

Accepted Manuscript

Licenced copy. Copying is not permitted, except with prior permission and as allowed by law.
© 2011 The Authors Journal compilation © 2011 Portland Press Limited

Biochemical Journal Immediate Publication. Published on 24 Jun 2011 as manuscript BJ20110750

Figure 2.

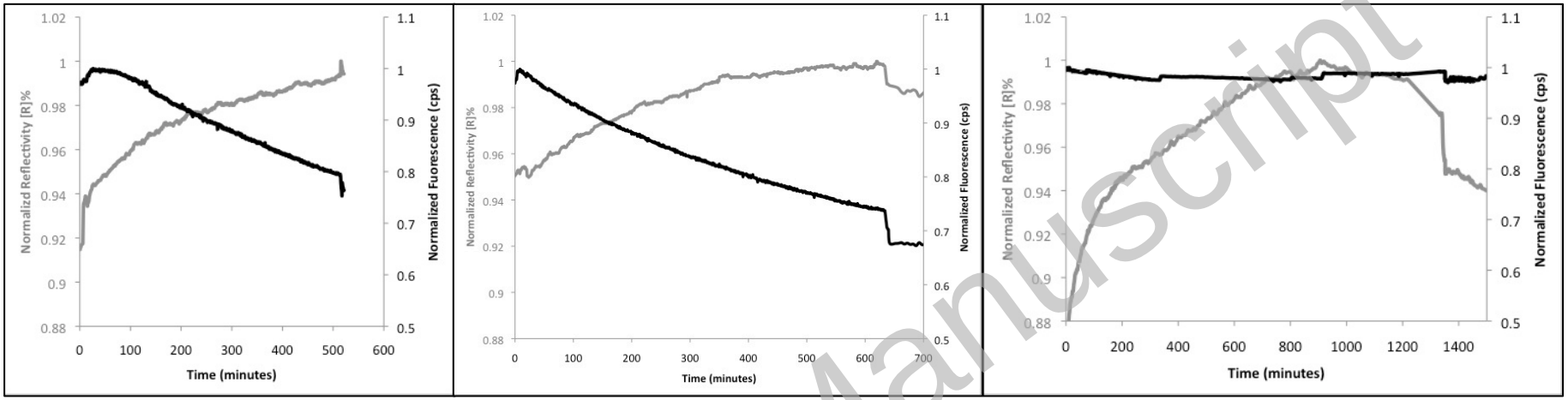

THIS IS NOT THE VERSION OF RECORD - see doi:10.1042/BJ2011

Accepted Manuscript

Licenced copy. Copying is not permitted, except with prior permission and as allowed by law.
© 2011 The Authors Journal compilation © 2011 Portland Press Limited

Biochemical Journal Immediate Publication. Published on 24 Jun 2011 as manuscript BJ20110750

Figure 3

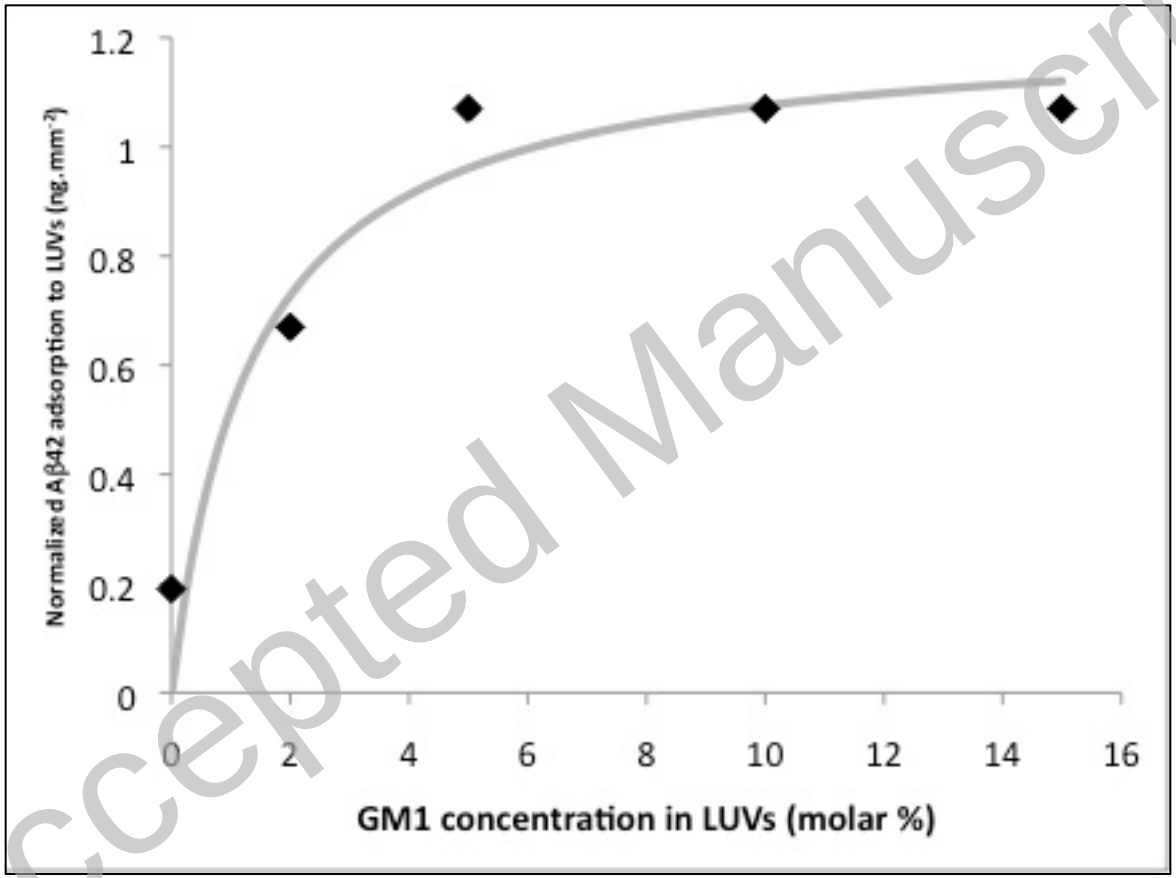

THIS IS NOT THE VERSION OF RECORD - see doi:10.1042/BJ20110750

Accepted Manuscript

Licenced copy. Copying is not permitted, except with prior permission and as allowed by law.
© 2011 The Authors Journal compilation © 2011 Portland Press Limited

THIS IS NOT THE VERSION OF RECORD - see doi:10.1042/BJ2011

Biochemical Journal Immediate Publication. Published on 24 Jun 2011 as manuscript BJ20110750

Figure 4

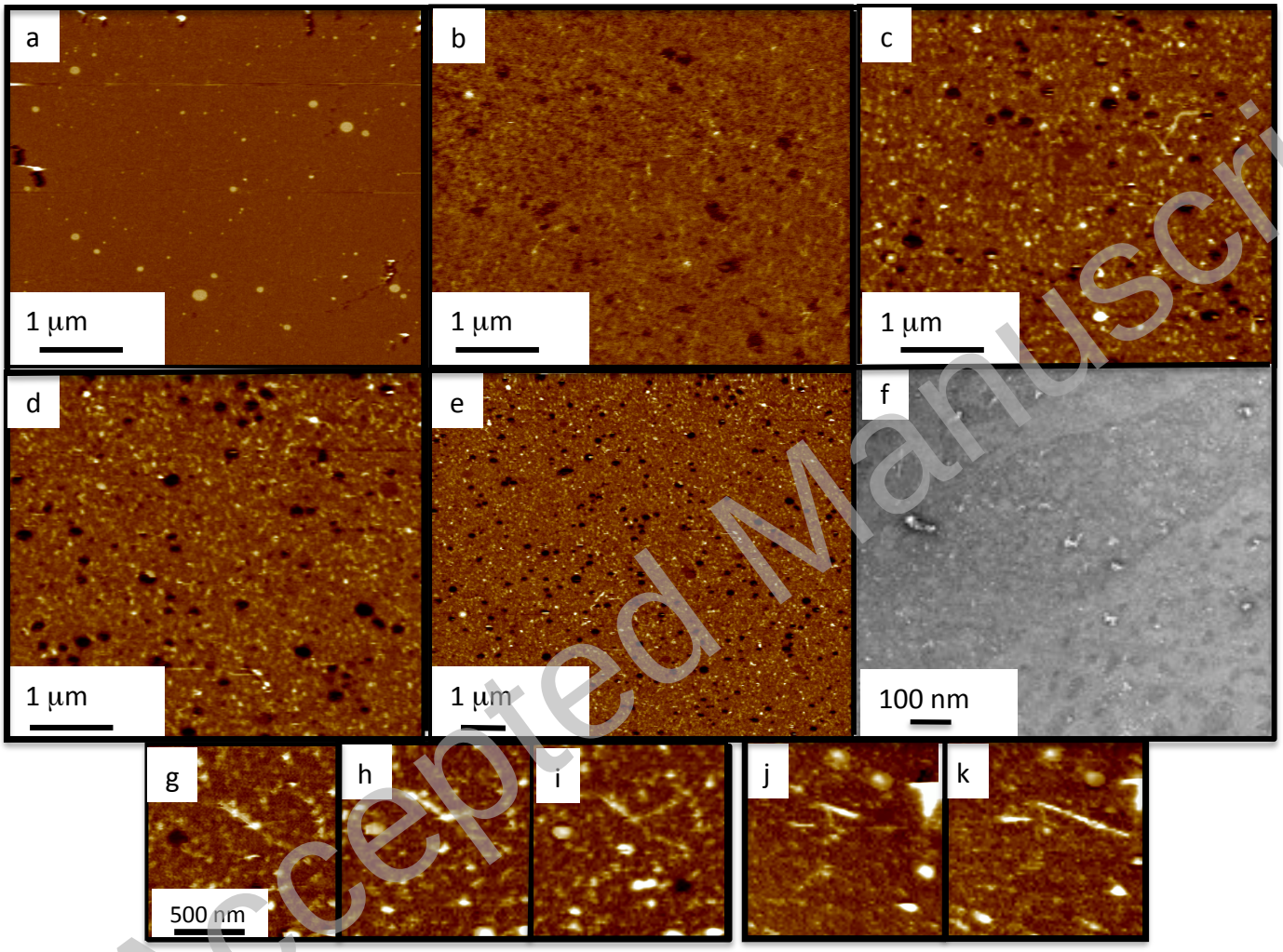

Accepted Manuscript

Licenced copy. Copying is not permitted, except with prior permission and as allowed by law.
© 2011 The Authors Journal compilation © 2011 Portland Press Limited

Biochemical Journal Immediate Publication. Published on 24 Jun 2011 as manuscript BJ20110750

THIS IS NOT THE VERSION OF RECORD - see doi:10.1042/BJ2011

Figure 5

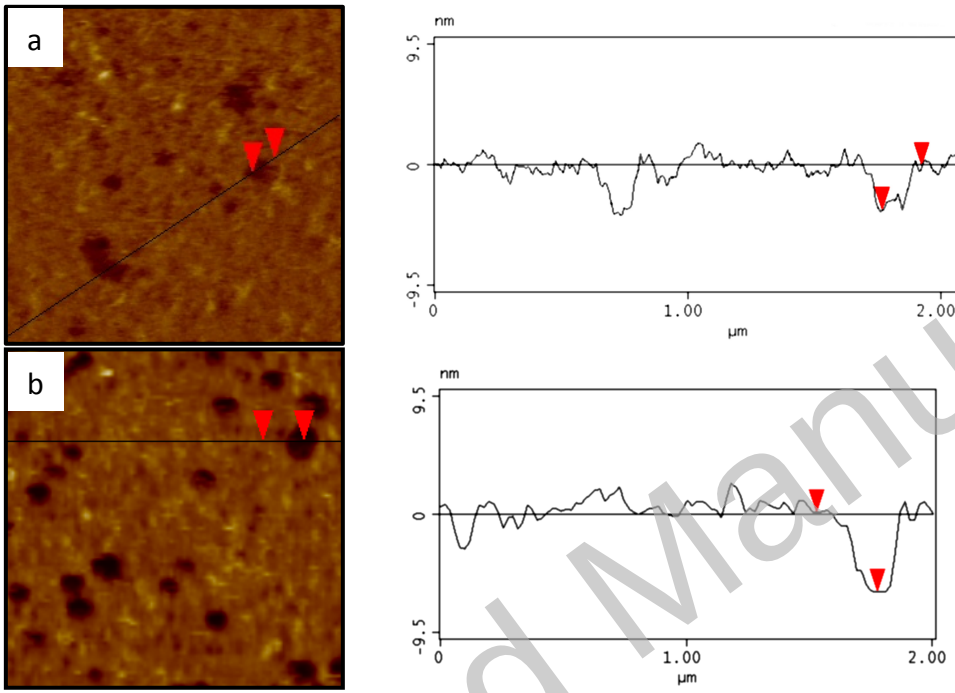

Accepted Manuscript

Licenced copy. Copying is not permitted, except with prior permission and as allowed by law.
© 2011 The Authors Journal compilation © 2011 Portland Press Limited